65 Rapid #: -1793356 **Ariel IP: 128.175.82.31**

Status	Rapid Code	Branch Name	Start Date
Pending	COF	EJournals	5/5/2008 7:10:56 AM

CALL #: http://condor.library.colostate.edu/sfxlcl3?url_ver=Z39.88-2004&ctx_ver=Z39.88-2004&ctx_enc=info:ofi/enc:UTF-8&rfr_id=info:sid/sfxit.com:opac_856&url_ctx_fmt=info:ofi/fmt:kev:mtx:ctx&sfx.ignore_date_threshold=1&rft.object_id=954925334699&svc_val_fmt=info:

LOCATION: **COF :: EJournals :: Cambridge University Press Journals Complete:Full Text**

TYPE: Article CC:CCL
JOURNAL TITLE: Robotica
USER JOURNAL TITLE:
COF CATALOG TITLE: Robotica
ARTICLE TITLE: Dubey, V.N., Crowder, R.M. and Chappell, P.H. "Optimal object grasp using tactile sensor and fuzzy logic"
ARTICLE AUTHOR:
VOLUME: 17
ISSUE: 6
MONTH:
YEAR: 1999
PAGES: 685-693
ISSN: 0263-5747
OCLC #: 9734967
CROSS REFERENCE ID: 42533432
VERIFIED:

BORROWER: **DLM :: Main Library**
PATRON: **Dubey, Venketeshwar Nath**
PATRON ID: vdubey
PATRON ADDRESS:
PATRON PHONE:
PATRON FAX:
PATRON E-MAIL: vdubey@udel.edu
PATRON DEPT: Mechanical Engineering
PATRON STATUS: vsch
PATRON NOTES:

Robotica (1999) volume 17, pp. 685–693. Printed in the United Kingdom © 1999 Cambridge University Press

Optimal object grasp using tactile sensors and fuzzy logic

Venketesh N. Dubey*, Richard M. Crowder** and Paul H. Chappell†

(Received in Final Form: May 22, 1999)

SUMMARY
Optimal control of fingertip force during grasping operation by multifingered robotic end effectors is an important consideration. Determination of optimal fingertip force is, however, very complicated due to the involvement of a number of contact parameters at the finger-object interface including the mass of the object and the frictional properties of the contact surfaces. Modelling of various contact parameters is computationally overloading, which may not be tenable in practical situations where objects of different mass and material are available. Also for an unknown and unstructured environment, these properties may not be known in advance. This paper presents a controller based on fuzzy logic which is capable of performing optimal grasp of objects without knowing their mass and frictional properties. The controller also accounts for stability and dynamic aspects of the grasp. The experimental results of the implementation are presented.

KEYWORDS: Object grasp; Tactile sensors; Fuzzy logic; Fingertip force; Robot controller.

1. INTRODUCTION
In the object handling operation by a robotic end effector, it is required to ensure a stable grasp without causing excessive gripping force to the object, and to minimise power consumption and to avoid possible damage to the object and the fingers. The grasp quality can be assessed by modelling the various material properties of the finger-object surface in contact and the applied force; this leads to complicated solutions.[1] In practice these are not valid for a different object-finger combination and for the changes in the fingertip force and moments during the handling operation. Also such grasp models do not offer real-time solution to the problem which can be implemented in practical systems. Apart from this, such systems cannot be used in an unknown and unstructured environment where objects of different mass and material are available, because the model relies on some predefined object properties. In order to offer a practical end effector with versatile grasping capability, the fingertip force needs to be controlled optimally in such a way that grasp is stable and is also capable of adapting dynamically to the external disturbances.

A number of existing grasp algorithms have been discussed,[2] however, it has been concluded that due to prohibitive computational complexities, none of the algorithms has been implemented in real-time systems. In an analysis of the multifingered hand for grasping and manipulation of objects, the force and moment balance equations are derived by considering the fingertip forces and moments, and the external forces and moments applied to the object.[3] Taking friction and joint torque constraints into account, the non-linear programming problem was reduced to linear programming by approximating the friction cone to a pyramid. In order to offer a real time solution to the problem, a sub-optimal method to compute grasping forces for a multifingered gripper has been developed.[4] The contact force has been decomposed into equilibrating and interaction forces and the solution was based on minimising every force component by the least square method. While describing the stiffness, strength and stability of a grasp, different contact conditions have been considered involving pointed, curved, soft and hard fingertips.[5] The rolling and deformation of the fingertips considerably complicated the analysis which did not allow real time computation of fingertip forces and moments.

Some other approaches considered use of tactile sensors to estimate the grasp quality based on detection of the contact parameters at the finger-object interface to obtain the changes in the contact parameter directly for real-time control. Grasp robustness from external disturbances has been shown by making use of force/torque sensors.[6] The algorithm however, required the data concerning the object strength, nominal value of contact force, coefficient of friction between fingertip and object surface. Dynamic grasp force control has been investigated based on tactile feedback.[7] The experiment required various parameters such as object mass, the static coefficient of friction at the contact, location of the centre of gravity. In the present paper, a controller has been described which uses tactile feedback from a photoelastic sensor, and is capable of forming optimal grasp for a variety of objects without knowing their mass and frictional properties. The experimental results of this implementation are also discussed.

2. THE PHOTOELASTIC SENSOR
In order to perform a successful handling operation, detection of applied force as well as object slip is necessary to estimate the condition of the grip. Tremblay et al.[8] have used a quartz crystal based accelerometer to detect the incipient slip. Howe and Cutkosky[9] have used strips of PVDF to measure the rate of change of stresses when object

* School of Computing Engineering and Technology, University of Sunderland, Edinburgh Building, Chester Road, Sunderland SR1 3SD (UK)
** Department of Electrical Engineering, University of Southampton, Southampton SO17 1BJ (UK)
† Department of Electrical Engineering, University of Southampton, Southampton SO17 1BJ (UK)

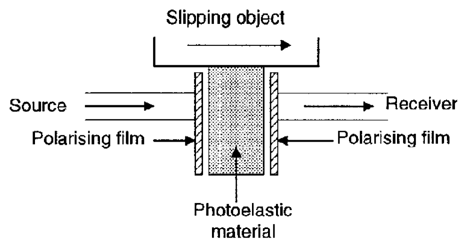

Fig. 1. Photoelastic slip and force sensor.

slides over it. Holweg et al.[10] have used rubber based tactile matrix sensor to detect slip. These sensors can only detect slip and are tested in idealised situations of forced slip.

A photoelasticity based sensor has been developed which is capable of detecting both applied force and the object slip. The developed sensor is based on the principle where a photoelastic material undergoing a change in applied stress, a corresponding change in the material's angle of polarisation occurs.[11,12] By passing polarised light through the photoelastic medium an effective change in the light intensity received can be observed. The outline of the sensor is shown in Fig. 1.

The developed sensor has been found to be sensitive down to a slip rate of 0.1 mm^{-1} for certain object material. In addition, it provides continuous slip signal when the object slides. A typical result from the slip sensor for an aluminium block of 0.1 kg slipping at a rate of 0.6 mm s^{-1} is shown in Fig. 2. In operation, the sensor initially detects the contact between the sensors and the object. If the object slips against the applied force, the sensor detects a cyclic slip signal in addition to the applied force.

The magnitude and frequency of the slip signal are a function of the contact materials and the rate of the slippage. In the developed sensor, the contact surface of the photoelastic material has been enhanced in such a way that it provides slip as well as applied force information.[13] Though the sensor is capable of detecting small slip rates, the dynamic range of the applied force detected by the sensor is found to be narrow (1.7 N). Consequently, only touch and minimum applied force event can presently be measured.

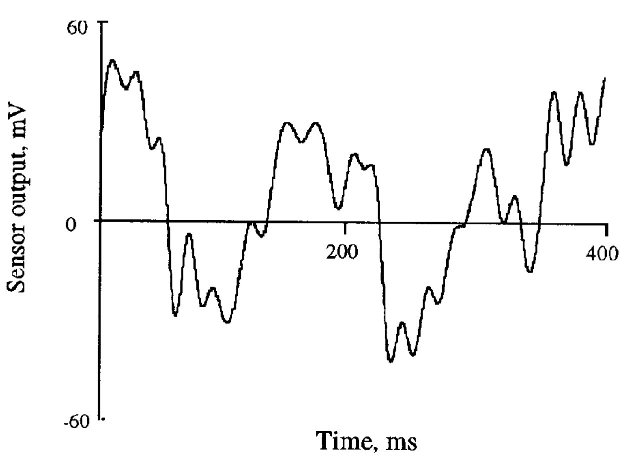

Fig. 2. Slip signal from the sensor.

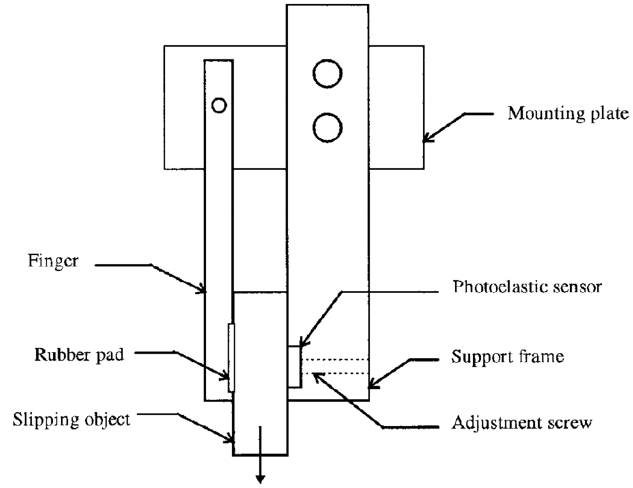

Fig. 3. The experimental test-rig.

3. THE EXPERIMENTAL SET-UP

The controller based on fuzzy logic is implemented in a test-rig with a simple finger. The schematic of the test-rig is shown in Fig. 3, which is operated by a DC motor. The maximum force that can be applied by the fingertip is 3.33 N. The support frame contains the photoelastic sensor. To enhance the flexibility of the controller, a force sensing resistor (FSR) is attached on the finger in addition to the photoelastic sensor so that the applied force of a wide dynamic range can be obtained.

4. THE FUZZY CONTROLLER

The fuzzy control for object grasp is implemented by considering two finger interaction inputs, namely the object

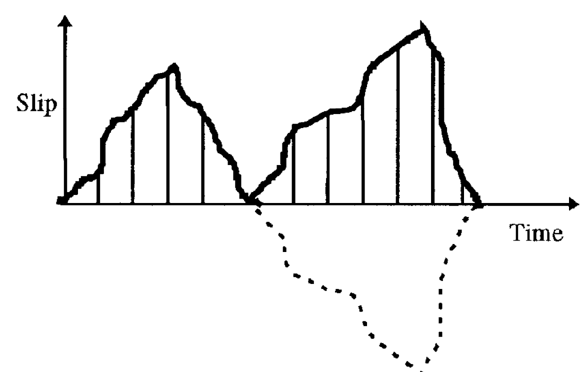

Fig. 4. Processing of the slip signal.

		fingertip force		
	T	S	M	L
s	AN	VS	S	M
l	S	S	M	L
i	M	M	L	VL
p	L	L	VL	VVL

Fig. 5. Fuzzy associative memory bank (FAM).

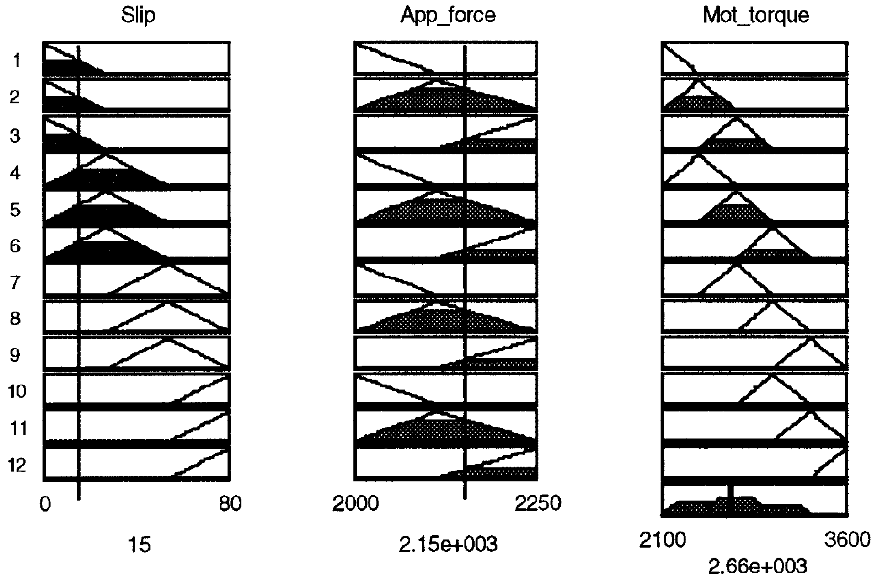

Fig. 6. The fuzzy inference engine.

slip and the applied force to the object. Individually these inputs give information on the object slip and the applied force to the object; however, the combined information can be used to form a grasp which applies minimum fingertip force without slipping the object. The current implementation is based on the Fuzzy Logic Toolbox,[14] operating under MATLAB. The package offers the flexibility of modelling and visualising the controller with any number of input and output under graphical user interface at each level. Once the modelling is completed and the output of the controller is tuned to a satisfactory level (by adjusting the primary fuzzy sets), the model file can be saved as a fuzzy inference system (FIS) file. This file can then be used by a fuzzy inference program with the required model-input to generate the expected output.

The modelling and generation of the FIS file is critical for implementing the controller since the output is completely based on this for the given inputs. The FIS file defines the knowledge base of the fuzzy system which has a data base and a fuzzy rule-base. The data base stores the information on the number of inputs and outputs, their range and the membership definition sets. The fuzzy rule-base contains

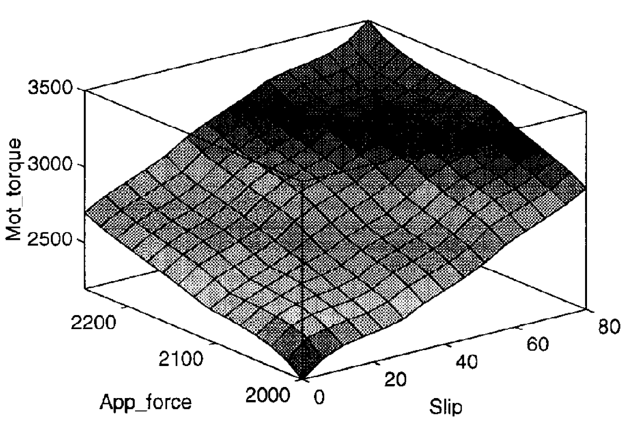

Fig. 7. The fuzzy rule surface.

the rules on which the control actions are based. The two input signals of object slip and the applied force are used in the controller which provide an output motor torque to hold the object. The input signals have been obtained from the developed photoelastic sensor and the FSR. The controller is designed to perform the grasping of various objects with a minimum fingertip force for each object and should be able to resist the object slip with extra holding force when the external disturbances exist.

In order to model and define the knowledge base of the controller, it is necessary that the range of operation of each input and output signals be experimentally determined. In this implementation the absolute values of each signal has been considered so that they can be related to each other in an easy linguistic way. Since the slip signal is AC in nature whose amplitude varies with the slip rate, it was necessary to process it before it could be used in the fuzzy inference system in the form of 'small' or 'large' slip. Figure 4 shows the sampling and signal processing of the slip signal to obtain its unidirectional peak value.

To obtain a pure applied force information from the photoelastic sensor, the signal from the sensor (which contains both AC and DC component corresponding to the slip and applied force) is filtered to provide the AC component. The de-coupled DC component is then obtained by subtracting the AC signal from the main signal.

The rules are defined in such a way to ensure stable grasp of object with minimum applied force. These rules are shown in the fuzzy associative memory bank (FAM), Fig. 5. The fuzzy set for the applied fingertip force and the slip information are arranged on the two sides of the table while the inference for the controlling motor torque is shown at the intersection of the two inputs (darker shades).

In the implementation, triangular membership functions have been chosen for each input and output signal. The primary fuzzy set for the applied force is taken to be small (S), medium (M) and large (L) while the fuzzy sets for the slip signal are almost nil (AN), S, M and L, and for the motor torque, these sets are very small (VS), S, M, L, very large (VL) and very very large (VVL). The motor torque has been divided into 6 primary sets to have different levels of force applied to the object for different combinations of the inputs.

Once the range of each input and output, and the primary fuzzy sets are defined, the controller can be modelled in the Toolbox. The rules in the FAM have been defined in such a way that at stable state (i.e. when the object slip is almost nil), the applied torque will remain only in the VS to M fuzzy sets. The remaining range of L to VVL is available as a reserved motor torque which can be applied to counter any external disturbances to the grasped object such as, the inertia force when a grasped object is moved by the manipulator or when the object is hit or pulled by an external force. It can be seen that the first row of FAM (with almost no slip) represents a class of minimum fingertip force, which can be applied to the object for different cases. A combination of the three primary sets, VS, S and M will be picked up by the controller depending on the mass of the object in grasp, since different holding forces are required to hold the object of different mass under the same frictional condition of the contacting surfaces. It has to be noted, however, that the controller accepts any value of inputs within fuzzy sets and due to the inherent interpolating nature of the fuzzy logic, it allocates an appropriate membership in each set for all the received inputs. This means regardless of the number of the primary fuzzy sets defined for each input, the controller can finely allocate membership to each input in different fuzzy sets.

The membership function of each input/output and the inference engine of the controller are shown in Fig. 6. The vertical lines (in the slip and the applied force fuzzy sets) indicate the two inputs to the controller which generates different memberships to various fuzzy sets. Based on the number of rules defined, the controller infers an appropriate motor torque. The inference engine shown in the figure is based on max-min operator and the centroid method of defuzzification.[15] With this structure of the controller, it applies minimum possible fingertip force to the object without knowing its mass and material properties, as will be shown in the following experimental results. The control rules with the even overlapping of the fuzzy sets can be viewed in the rule surface, Fig. 7.

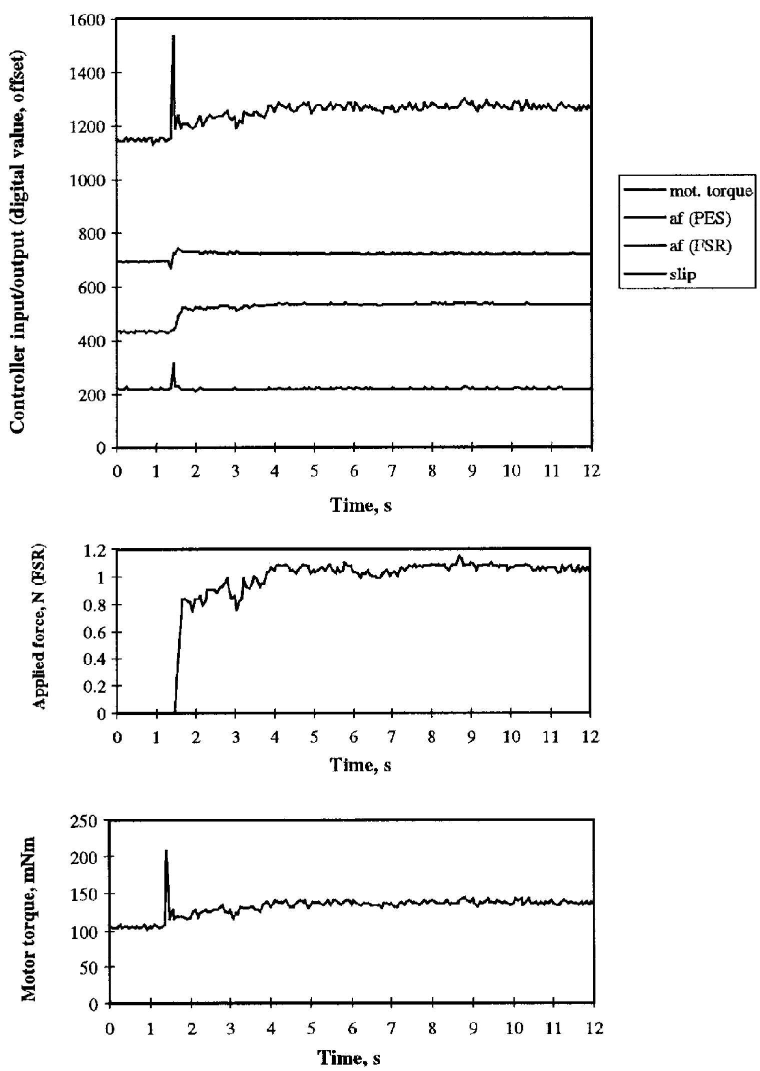

Fig. 8. Controller characteristics for no-object, no-slip situation.

5. EXPERIMENTAL RESULTS

The implementation of fuzzy controller has been tested. The input and output signals are presented as separate plots. Fig. 8 shows the initial condition of the system where the finger is moved to grasp an object, however, in this case no object is available for the grasp. This means the finger is moved to touch the sensor and no object slip was recorded. As shown in the upper plot, the four signals from top to the bottom are motor torque, applied force signal from the photoelastic sensor (PES), applied force signal from the FSR (which has been used in the implementation), and finally the slip signal. These digital signals have been offset to bring them together for comparison purposes and to see the effect of change in the output with respect to the inputs. In the lower plots, the applied force (FSR) and the motor torque have been converted to the actual units based on the FSR calibration and the motor specification. It can be clearly seen that under no-object, no-slip conditions, the motor generates a constant torque of 125 mNm. The applied fingertip force recorded by the FSR is approximately 1 N. The initial low values of input/output signal until 1.5 s show the time taken by the finger to make contact with the sensor. When the finger makes first contact with the sensor, it receives an impact which is recorded by the photoelastic sensor as a high slip signal as well as a high applied force (Fig. 8), consequently the applied motor torque is very high (200 mNm). However, as the contact is established the slip signal dies out and the motor torque and the applied force comes to a steady state. It can be seen that the initial response of the FSR is acceptable but it slowly attains a steady state after around 2.5 s from the first contact. It can be further seen that the photoelastic sensor follows the similar trend for the applied force as shown by the FSR with a smaller range. The time scale shown on the abscissa is the duration for which the experiment was conducted and is different for each experiment. Though the data acquisition card runs at 100 KHz, the overall loop frequency using the fuzzy inference system is found to be 16 Hz. This can, however, be improved by properly customising the fuzzy inference system. In each of the following experiments (for grasping

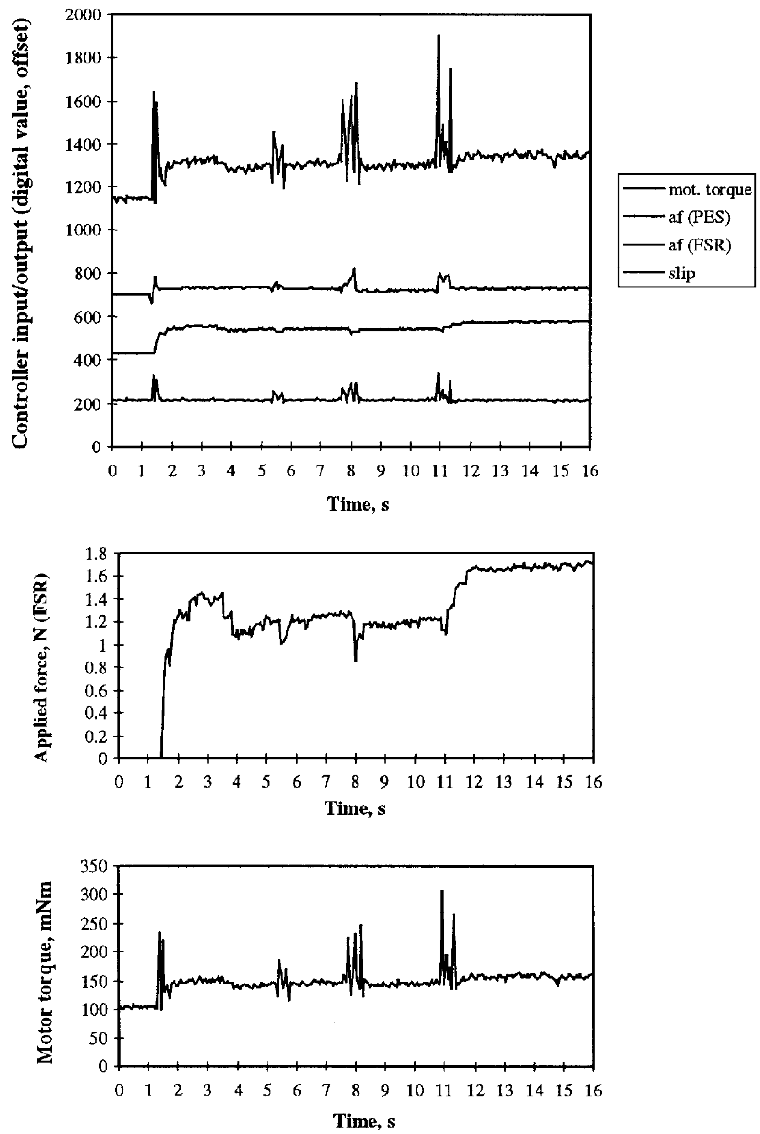

Fig. 9. Controller characteristics for holding a stainless steel object of 0.063 kg.

objects of different mass) two aspects have been studied. Firstly, to find the holding force and secondly to evaluate the dynamic stability of the grasp by applying an external force to pull the object from the grip.

Figure 9 shows the controller characteristics for holding a stainless steel object of 0.063 kg. It can be seen that due to the initial slip of the object more than one spike appeared in the slip signal which in combination with the applied force from the FSR, produced an output motor torque of 250 mNm. The force applied tries to arrest the object slip and when the slip subsides the motor torque drops to 140 mNm. Accordingly the applied fingertip force decreases from 1.4 N to a steady state value of 1.25 N. This applied force can be compared with the previous case of no-object, no-slip, when it was found to be just 1 N. Thus the applied force increases when there is an object in grasp. This applied force, however, may not be the minimum fingertip force for holding the object since the applied motor torque is based on the initial slip signal (which is very high due to the initial finger contact) and the initial applied force. Even when the slip completely dies out, the motor torque may remain in a higher state than the minimum and so is the case for the applied force. This can be better explained with the help of rules defined in FAM. Since for no slip condition, the applied force can acquire any combination of VS, S or M status (see the first row of FAM). If it is assumed that in the beginning the object is slipping over the sensor, and to arrest the slip the controller continuously increases the motor torque. At equilibrium, the motor torque will be just sufficient to stop the object slip, say this state of the applied force is represented by some levels in the VS and S primary fuzzy sets. However, if it is imagined that when the object is slipping, a higher motor torque (than required) is applied instantly, then also the object slip is arrested but this is not the case of minimum fingertip force applied to the object.

In this case the applied force may have some memberships in S and M primary fuzzy sets, which again is a stable state with respect to the first row of FAM. Thus there could be a similar situation during initial contact, when the slip sensor records a very high slip and accordingly the controller supplies a high motor torque which immediately arrests the object slip. Possibly the applied fingertip force in

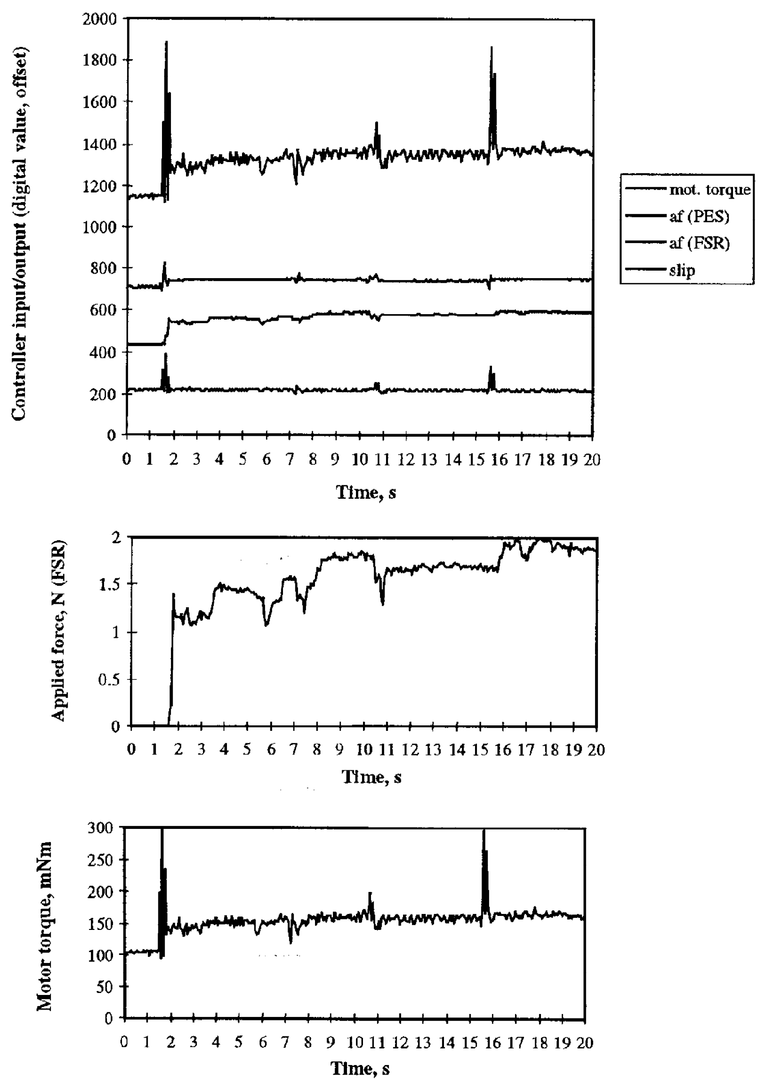

Fig. 10. Controller characteristics for holding a brass object of 0.075 kg.

this situation may not be minimum. Such conditions lock the controller at a higher state and cannot come back to a minimum level by itself if the fingertip force is not relaxed.

In order to test the dynamic stability of the system, the object is perturbed producing the slip signal during the time interval of 5 s to 6 s (Fig. 9). At the same time interval, the applied force is seen to decrease. This is due to the instantaneous contact lost by the finger due to the perturbation, since the FSR is mounted on the flexible finger. The resultant effect of the applied force and the slip signal provides the motor torque which is almost the same as the previous value of 1.25 N after the slip has subsided. The applied force signal from the photoelastic sensor is more noticeable because it has a dynamic force sensing capability with a very high response. Further the applied force is seen to increase at the time of perturbation, since the photoelastic sensor is mounted on a rigid support which does not lose contact during perturbation. The sensor material gets stressed by the perturbation and it regains the previous condition after the perturbation has vanished. Due to slow response and that the FSR is mounted on the moving finger of the test-rig, this event is not exhibited by the FSR.

It can be further seen from the same figure that when the object is given a bigger perturbation (slip) in the time interval of 7 s to 9 s, a bigger loss of contact at FSR appears.

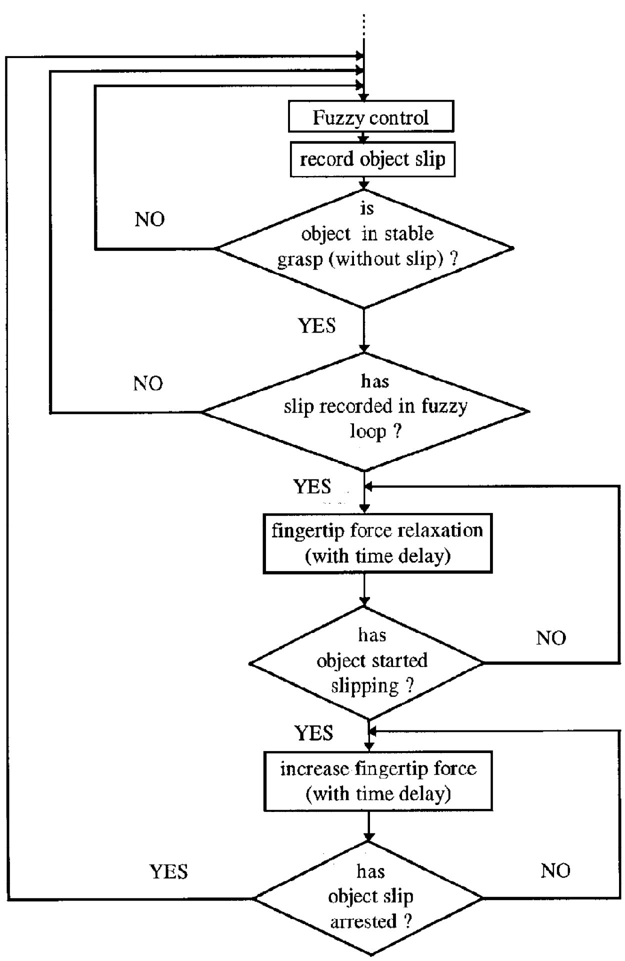

Fig. 11. The force relaxation algorithm.

And as a result of the two large inputs, the output torque increases quickly to the extent of 250 mNm to arrest the object slip. However, as soon as the slipping object attains equilibrium, the applied force from the FSR is found to drop from the previous value. This means that the combination of the applied force and the slip in the previous case was not offering a minimum motor torque and the resulting applied force, for the same reason (as discussed earlier) of motor torque attaining higher state. The new fingertip force during the steady state, in the time interval of 8 s to 11 s is found to be 1.2 N.

When the object is given a still bigger perturbation at 11 s, the slip is seen to be very large and the output motor torque to control this increased to 300 mNm. This applies a higher fingertip force of 1.7 N and stays there which means that the applied force moves from one state to the other state of the primary fuzzy sets and the object attains stability at this higher force. Thus, it can be concluded that for a range of object slip (external disturbances), the controller is capable of holding the object exhibiting the dynamic stability of the grasp. For a stainless steel object of 0.063 kg, the minimum holding force is found to be 1.2 N. This can be used to obtain the value of average coefficient of friction between the contacting surfaces of the object with the finger (which is covered by a soft foam material to protect the FSR from abrasion) and the sensor metallic surface. This is found to be 0.52.

The experiment was repeated with a brass object of 0.075 kg. The results are shown in Fig. 10. The minimum fingertip force required to hold the object is 1.45 N under a motor torque of 150 mNm. If the value of the coefficient of friction in the previous experiment is taken to be approximately the same for this experiment, the mass of the object can be back calculated, which comes out to be 0.0768 kg. This is fairly close to the actual mass of the object. This shows the fineness of the controller which applies fingertip force according to the mass and material of the object.

In order to keep the fingertip force in all situations to a minimum, a force relaxation algorithm has been developed (Fig. 11). The algorithm operates continuously in a closed loop within the fuzzy control algorithm and records object slip event.

As soon as a stable grasp is achieved and a slip has been recorded in the fuzzy loop, the control is passed to a force relaxation algorithm. In this loop, the motor torque is relaxed in small steps until the object starts slipping. At this condition, the relaxation loop is broken and the control is passed to another loop where the motor torque is increased in small steps. The force increase arrests the object slip quicker than the release of object during relaxation due to high static inertia. Under this situation the fingertip force is just above the minimum to hold the object. At this condition the control is passed back to the fuzzy loop. A time delay of few seconds (typically 2–4 s) can be incorporated in the force relaxation and the increment loops for the sensor to attain stability and for a gradual change of the fingertip force.

In Fig. 12, the controller characteristics for the 0.075 kg brass object have been shown with force relaxation provision. After the initial grasp, the object has been

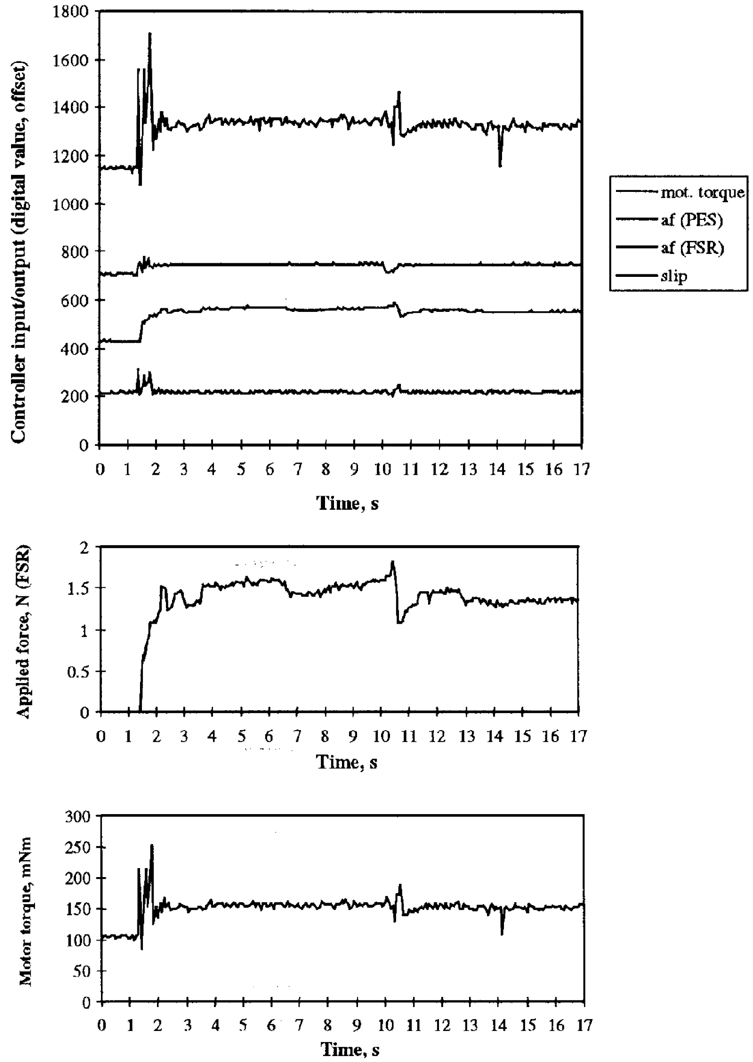

Fig. 12. Controller characteristics for holding a brass object of 0.075 kg with fingertip force relaxation provision.

perturbed in the time interval of 10 s to 11 s. It can be seen that the initial fingertip force decreases from 1.5 N to 1.4 N due to the loss of contact and the following backward level-shifting of the inputs in the primary fuzzy sets caused by the perturbation. The force relaxation comes into effect at 14 s; however, it does not change the fingertip force level since it has already attained the minimum during the previous slip (perturbation). In the majority of the test-run for fingertip force relaxation, it has been found that the finger is able to achieve the minimum force. However, in some cases, the object grasp is completely lost and the object falls. This is due to high frictional property of the contact pad at the fingertip which does not allow the object to slip even when the grasping force is less than the minimum, the motor torque during relaxation reaches very low level when the object falls before breaking the loop. Under this situation the fuzzy control comes into operation only after slipping the object, which records a slip due to the loss of contact.

However, if the object mass is heavier, such situations will not occur and the object will start slipping just below the minimum fingertip force allowing the algorithm to perform satisfactorily. This has not been investigated since the motor used was not capable of holding heavier mass.

From Fig. 12 it can be further seen that the controller applies almost the same motor torque of 150 mNm and the fingertip force of 1.5 N (before the slip has occurred) as shown in Fig. 10 for the same brass object of 0.075 kg. This means that the controller exhibits a consistent behaviour. Further, the controller applies different motor torque and the resulting different fingertip force of 1 N, 1.2 N and 1.45 N for different conditions of object in grasp as shown in Figs. 8, 9 and 10, respectively. This indicates that the controller is capable of finely controlling the fingertip force depending on the mass and material of the objects. These experiments were also conducted with the articulated finger, used in the design of a number of end effectors developed at the University of Southampton;[16] the controller exhibited a similar behaviour.

6. DISCUSSION AND CONCLUSIONS

The implementation of fuzzy control and the associated expert rule for the optimal grasp of objects have been discussed. The results of the fuzzy control implementation have been presented to validate that the controller is able to form optimal grasps with minimum required fingertip force for different objects without knowing their mass and the frictional properties. The controller is found to respond quickly to the external disturbances providing extra force at the fingertip to offer dynamic stability to the grasp. This offers a novel capability to the controller which is particularly useful for operating the end effector in an unknown and unstructured environment where the mass and material properties of the object may not be known in advance.

Since the controller relies on the slip and the applied force information, it requires to ensure that the finger has made full contact with the object and that the slip and the applied force information can be extracted from the employed tactile sensors. Although the controller designed operates when the contact with object has been established, however, the relaxation algorithm can account for the transitional disturbances between contact and no-contact situations. The controller attempts to emulate the grasping capabilities of the human hand which does not require a priori knowledge of the object properties and is capable of forming optimal grasp in various cases. A complete model of the controller for a three-fingered end effector has been simulated for equilibrium and dynamic stability of the grasp based on the developed fuzzy rules.[13] The three dimensional model satisfies the equilibrium criterion for the grasped object, in addition it also accounts for the positional imbalances arising due to uneven spread of the fingers over the object. Currently the manipulation of objects has not been pursued, however, similar expert rules can be generated based on the slip motion of the fingers over the grasped object.[17] A controller with these capabilities will be useful in a range of applications including prosthetics and telerobotics.

Acknowledgements

This research has been supported by the Faculty of Engineering and Applied Science, University of Southampton, Department of Electrical Engineering, University of Southampton and the Overseas Research Student award from the UK Committee of Vice-Chancellors and Principals.

References

1. M.R. Cutkosky and P.K. Wright, "Friction, stability and the design of robotic fingers" *Int. J. Robotic Research* **5**, No. 4, 20–37 (1986).
2. K.B. Shimoga, "Robot grasp synthesis algorithms: A survey", *Int. J. Robotics Research* **15**, No. 3, 230–266 (1996).
3. J. Kerr and B. Roth, "Analysis of multifingered hands" *Int. J. Robotics Research* **4**, No. 4, 3–17 (1986).
4. V. Kumar and K.J. Waldron, "Sub-optimal algorithms for force distribution in multifingered grippers" *IEEE Trans. Robotics and Automation* **5**, No. 4, 491–498 (1989).
5. M.R. Cutkosky, *Robotic Grasping and Fine Manipulation* (Kluwer Academic Publishers, Boston, 1985).
6. A. Bicchi, J.K. Salisbury and P. Dario, "Augmentation of grasp robustness using intrinsic tactile sensing", *Proc. of the IEEE Intl. Conf. on Robotics and Automation* (1989) pp. 302–307.
7. H. Maekawa, K. Tanie and K. Komoriya "Tactile feedback for multifingered dynamic grasping", *IEEE Control System Magazine* 63–72 (1997).
8. M.R. Tremblay, W.J. Packard and M.R. Cutkosky, "Utilising sensed incipient slip signals for grasp force control" *Proc. Japan-USA Symp. on Flexible Automation* (1992) **Part 1**, pp. 1237–1243.
9. R.D. Howe and M.R. Cutkosky, "Sensing skin acceleration for slip and texture perception" *Proc. of the IEEE Intl. Conf. on Robotics and Automation* (1989) pp. 145–150.
10. E.G.M. Holweg, H. Hoeve, W. Jongkind, L. Marconi, C. Melchiorri and C. Bonivento "Slip detection by tactile sensors: algorithm and experimental results" *Proc. IEEE Intl. Conf. on Robotics and Automation* (1996) pp. 3234–3239.
11. F. Kvasnik, B.E. Jones and M.S. Beck, "Photoelastic slip sensors with optical fiber links for use in robotic grippers" *Institute of Physics Conf. on Sensors*, Southampton, UK (1985) pp. 58–59.
12. P. Dario, D. Femi and F. Vivaldi, "Fiber-optic catheter-tip sensor based on the photoelastic effect" *Sensors and Actuators* **12**, 35–47 (1987).
13. V.N. Dubey "Sensing and control within a robotic end effector", *PhD thesis* (University of Southampton, UK, 1997).
14. J.S. Roger Jang and N. Gulley, *Fuzzy Logic Toolbox* (The Math Works, Inc., USA, 1995).
15. B. Kosko *Neural Networks and Fuzzy Systems* (Prentice Hall International editions, USA, 1992).
16. R.M. Crowder, "Special purpose multifingered robotic end effectors" *Proceedings, 38th Conference on Remote Systems Technology* (1990) **Vol. 2**, pp. 52–58.
17. T. Yoshikawa, Y. Yokokohji and A. Nagayama, "Object handling by three-fingered hands using slip motion" *Proc. of the IEEE/RSJ Intl. Conf. on Intelligent Robots and Systems* (1993) pp. 99–105.